

000 001 002 003 004 005 006 007 008 009 010 011 012 013 014 015 016 017 018 019 020 021 022 023 024 025 026 027 028 029 030 031 032 033 034 035 036 037 038 039 040 041 042 043 044 045 046 047 048 049 050 051 052 053 TASTE: TEXT-ALIGNED SPEECH TOKENIZATION AND EMBEDDING FOR SPOKEN LANGUAGE MODELING

Anonymous authors

Paper under double-blind review

ABSTRACT

Recent efforts target spoken language models (SLMs) that not only listen but also speak for more natural human-LLM interaction. Joint text-speech modeling is a promising direction to achieve this. However, the effectiveness of recent speech tokens for joint modeling remains underexplored. To address this, we introduce Text-Aligned Speech Tokenization and Embedding (TASTE), a method that directly addresses the modality gap by aligning speech token with the corresponding text transcription during the tokenization stage. We propose a method that can achieve this through an attention-based aggregation mechanism and with speech reconstruction as the training objective. We have conducted extensive experiments to demonstrate that TASTE can preserve essential paralinguistic information while dramatically reducing the token sequence length. Moreover, TASTE enables straightforward joint spoken language modeling by using Low-Rank Adaptation on the pre-trained text LLM. Our experimental results show that joint modeling with TASTE outperforms other pre-trained SLMs in tasks such as speech continuation and likelihood-based next-speech selection, showcasing its effectiveness. To our best knowledge, TASTE is the first end-to-end approach that utilizes a reconstruction objective to learn a joint tokenization and embedding tailored for text-speech spoken language modeling. Our demo, code, and models are available at <https://anonymous-ai-work.github.io/TASTE-SpokenLM.github.io>.

1 INTRODUCTION

Spoken language modeling (SLM) is an intriguing direction nowadays that aims at creating models that can not only listen but also *speak* (Lakhotia et al., 2021; Nguyen et al., 2023; Défossez et al., 2024; Fang et al., 2024; Arora et al., 2025). Typically, building an SLM requires two stages: first, deriving speech tokenizations; second, training a language model based on the speech tokens. For the speech tokens, previous approaches either apply self-supervised learning (SSL) representations following by discretization techniques (Baevski et al., 2020; Lakhotia et al., 2021; Nguyen et al., 2023; Hassid et al., 2023) or reuse units from neural codec models like EnCodec and SoundStream (Défossez et al., 2023; Zeghidour et al., 2021; Kumar et al., 2023; Siuzdak et al., 2024). Although autoregressive modeling with these speech tokens shows great potential in text-to-speech (TTS) (Wang et al., 2023; Xin et al., 2024a; Kim et al., 2024; Chen et al., 2024), previous SLMs that model only speech tokens (Lakhotia et al., 2021; Nguyen et al., 2023) have been shown to lack semantic fidelity (Lin et al., 2024).

To bridge this gap, one promising direction is to leverage text—which is rich in semantics—during spoken language modeling. TWIST (Hassid et al., 2023) shows that SLMs can benefit from initializing with text LLMs. Building on this idea, recent work has shifted toward joint text–speech modeling to enhance semantic coherence in generated speech. Such approaches typically adopt a hybrid decoding scheme that generates both text and speech tokens. However, combining the two modalities introduces a length mismatch, since speech token sequences are usually much longer than their textual counterparts. Common remedies include interleaving text and speech tokens (Nguyen et al., 2025) or inserting padding to synchronize sequence lengths (Défossez et al., 2024; Xie & Wu, 2024a; Fang et al., 2024; Xie & Wu, 2024b), but these solutions rely on additional alignment procedures or heuristic rules, making joint modeling more complex.

As hybrid text–speech decoding becomes the prevailing paradigm for joint SLM (Défossez et al., 2024; Xie & Wu, 2024a; Fang et al., 2024; Li et al., 2025; Xie & Wu, 2024b), the design of speech

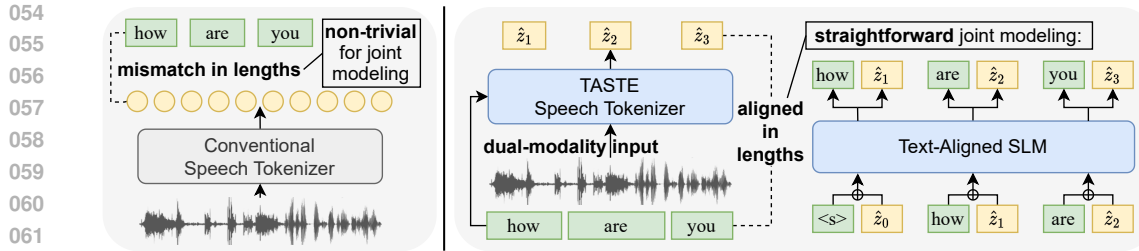


Figure 1: **The concept overview.** Conventional methods extract speech tokens solely from speech, inevitably carries overlapped information with text tokens and induces length-mismatch problem when conducting joint text-speech modeling. By taking dual modalities as input, we generate speech tokenization that is aligned with text, facilitating straightforward and effective joint modeling.

tokens should be reconsidered in light of this setting. This motivates the development of more effective joint tokenization methods, which can be derived under the following two considerations: 1) a speech token should avoid redundantly encoding text content—already captured by the text tokens—and instead focus on conveying paralinguistic information; and 2) a straightforward one-to-one correspondence between text and speech tokens is preferable, as it allows SLMs to generate a text token and a speech token simultaneously without any heuristics or explicit alignments applied, mitigating the length mismatch issue during the tokenization stage.

In this work, we introduce Text-Aligned Speech Tokenization and Embedding (TASTE), a special type of joint tokenization tailored for text-speech joint spoken language modeling. By acknowledging that the length mismatch introduces additional complexity in joint modeling, we develop our speech token to be aligned with its corresponding text transcription tokens. To achieve this, we first obtain the textual transcription of a speech with the ASR model; then we derive the speech token based on the transcription through a specialized cross-attention mechanism for speech reconstruction. Note that the full process can be accomplished in an end-to-end manner, with no explicit speech-text alignment required. Unlike previous speech tokens that are developed under a fixed stride with fixed down-sampling rate, our speech token has dynamic frequency as it is text-aligned. Figure 1 shows an overall concept of TASTE, illustrating how our joint tokenization allows effective joint modeling.

To evaluate the effectiveness of TASTE, we first conduct extensive experiments on speech reconstruction. Our results on LibriSpeech (Panayotov et al., 2015) show that TASTE not only resynthesizes speech in high quality, but also retains similarity to the original speech. TASTE achieves high-end reconstruction at an extremely low bit rate (~ 150 bps); while the other comparable methods are often more than thousands of bps. We attribute the efficiency to the involvement of text tokens during encoding and decoding, and our speech tokens focus on carrying paralinguistic information, which is backed up by the demonstration that TASTE allows simple text-aligned speech editing. By exchanging the partial text-aligned speech tokens from two different utterances with the same content, we demonstrate that the paralinguistic information such as duration and tone can be exchanged precisely following the words being exchanged, resulting in natural edited speech.

On the other hand, we demonstrate that TASTE successfully allows effective spoken language modeling. We perform straightforward joint modeling with TASTE under Low-Rank Adaptation (Hu et al., 2021). We first perform speech continuation experiments with 3-second speech prompts given. The evaluation is three-fold. We use GPT-4o for evaluating the semantic aspect; UTMOS (Saeki et al., 2022) for the acoustic aspect; and the human listening test for the general evaluation. Results show that our SLMs not only generates natural, meaningful speech continuations, but also outperforms the other 7B pre-trained SLMs across all the continuation evaluation aspects with 1.3B parameters. We also evaluate our SLMs on two benchmarks, SALMON (Maimon et al., 2024) and StoryCloze (Hassid et al., 2023) and our results show that our SLMs achieve comparable performance compared to the other text-speech joint modeling methods. Moreover, we show that our pretrained SLM can perform spoken question answering under the few-shot scenario.

In summary, we derive TASTE, a specialized tokenization approach for text–speech spoken language modeling. By aligning speech tokens with their text counterparts, TASTE provides a simple yet effective form of joint tokenization. Our results highlight joint tokenization as a key factor in joint modeling, offering a new perspective that may foster further research into more effective designs.

108

2 RELATED WORK

110 Recent SLMs often require speech tokenization to conduct language modeling with the next prediction
 111 objective as the text LLMs. Unlike text, the speech signal is continuous and lengthy, making it difficult
 112 to derive proper speech tokenization for spoken language modeling. Common approaches may utilize
 113 self-supervised learned (SSL) speech models followed by quantization techniques to extract speech
 114 tokens (Baevski et al., 2020; Hsu et al., 2021; Lakhotia et al., 2021; Hassid et al., 2023; Nguyen
 115 et al., 2025). In addition, audio or speech codec models have also been used for tokenization in recent
 116 SLMs (Zeghidour et al., 2021; Défossez et al., 2023; 2024; Zhang et al., 2024). These models are
 117 designed for resynthesis, where the speech decoders are jointly learned with the encoders, making
 118 them easy to use for developing SLMs.

119 With speech tokenization, GSLM (Lakhotia et al., 2021) first demonstrates the possibility of building
 120 an SLM that can generate speech. TWIST (Hassid et al., 2023) further shows that SLM can benefit
 121 from initialization with the text-pretrained LLM. With regard to the huge success of text-only LLMs,
 122 recent work shifts the focus towards joint speech-text modeling (Défossez et al., 2024; Xie & Wu,
 123 2024a). Challenged by the modality gap between speech and text tokens, different techniques are
 124 introduced to facilitate joint modeling. Spirit LM (Nguyen et al., 2025) adopts an interleaving
 125 strategy; moshi (Défossez et al., 2024) trains its own tokenizer with a reduced token frequency.
 126 Moreover, delayed or sequential generation are introduced for joint modeling (Xie & Wu, 2024a).

127 Despite the increasing demand of joint speech-text modeling, we do not find any work discussing
 128 the effectiveness of current speech tokenization for it. Moreover, the speech token is often derived
 129 with speech or audio-only data¹. Nonetheless, we observe that recent work is trying to mitigate
 130 the modality gap by reducing speech token frequency (Défossez et al., 2024; Zeng et al., 2024) or
 131 conducting additional training stage for text-speech alignment (Xie & Wu, 2024a). This motivates us
 132 to design a speech tokenization that is directly aligned with its text counterpart, tackling the mismatch
 133 issue during the tokenization stage.

134 In TASTE, we utilize a specialized mechanism based on attention to aggregate the encoder represen-
 135 tations. We clarify that the text-speech cross-attention mechanism has also been used for fine-grained
 136 control of TTS. More specifically, Chen & Rudnicky (2022) propose content-style cross-attention to
 137 indicate their text-speech cross-attention mechanism that enables style transfer in TTS. Although both
 138 utilize a specialized text-speech cross-attention mechanism, the design choices and problem formula-
 139 tions are completely different. We attribute of our main novelty to inventing a text-aligned speech
 140 tokenization and embedding for joint spoken language modeling, and the text-speech cross-attention
 141 mechanism is considered and shown to be a clean and effective way of achieving it.

142

3 METHOD

143 We propose text-aligned speech tokenization and embedding (TASTE) to facilitate effective joint
 144 speech-text spoken language modeling. Here, we first introduce how we derive our joint tokenization
 145 in Section 3.1, and then discuss how we use TASTE for spoken language modeling (§ 3.2).

146 As depicted in Figure 2, TASTE is comprised of the two main components: the text-aligned speech
 147 tokenizer (§ 3.1.1) that produces the text-aligned speech tokenization; and the speech decoder (§ 3.1.2)
 148 to *reconstruct* speech based on the text token and the TASTE speech token aligned with it. The
 149 training objective of speech reconstruction is described in Section 3.1.3.

150

3.1 BUILDING TASTE

151

3.1.1 TASTE SPEECH TOKENIZER

152 In TASTE, the speech tokenizer, denoted as $\text{Tokenizer}(\cdot)$, is designed to generate the text-aligned
 153 speech tokenization and embedding with the speech-text pair $X = (\mathbf{u}, \mathbf{v})$ taken as input, where
 154 \mathbf{v} represents the textual transcription of the speech utterance \mathbf{u} , which can be easily obtained
 155 through an automatic speech recognition (ASR) system. Recent developments in robust and efficient
 156 ASR (Radford et al., 2023; Gandhi et al., 2023) allow us to focus on discussing how to derive the
 157

158 ¹An exception is CosyVoice (Du et al., 2024a). We discuss it in Section 3 since it is related to our method.

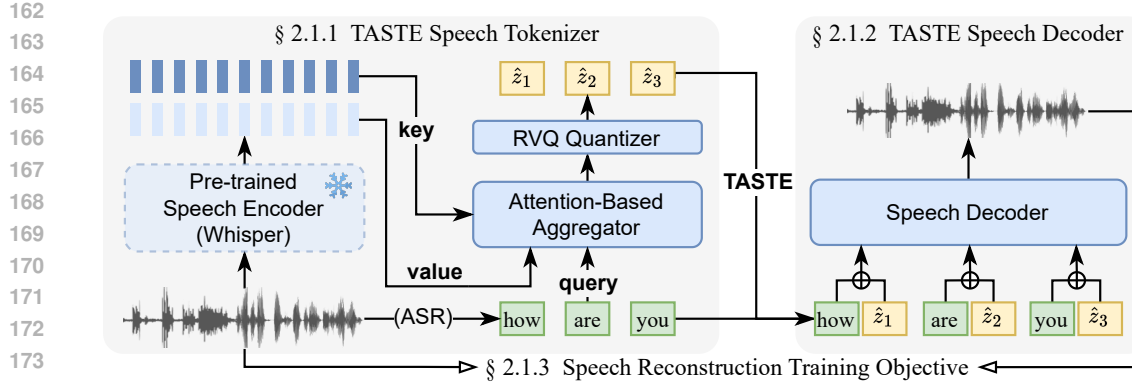


Figure 2: **The overall framework of our text-aligned speech tokenization and embedding.** The left side illustrate the process of obtaining the TASTE tokenization \hat{z} , detailed in Section 3.1.1; while the right side demonstrate how we reconstruct the speech with TASTE (Section 3.1.2). The training objective for our speech reconstruction is discussed in Section 3.1.3.

text-aligned speech token effectively by assuming that v is of sufficient quality. The TASTE speech tokenizer is composed of three major components: an *encoder*, an *aggregator*, and a *quantizer*.

The encoder $\text{Encoder}(\cdot)$ contains L layers of Transformer (Vaswani et al., 2017) encoder blocks and is used to extract high-dimensional speech representation. We employ the pre-trained Whisper ASR encoder (Radford et al., 2023) as our speech encoder, and it is frozen during training. For an input speech utterance u , the encoder produces a sequence of hidden states from each layer $[\mathbf{h}^{(1)}, \mathbf{h}^{(2)}, \dots, \mathbf{h}^{(L)}]$. In our experiments, we retain the *last* hidden layer representation $\mathbf{h}^{(L)}$ and the *shallow* representation $\mathbf{h}^{(l)}$ from the first half of the hidden representations of the encoder for later usage, denoted as:

$$\mathbf{h}^{(L)}, \mathbf{h}^{(l)} = \text{Encoder}(u), \quad \text{where } 1 \leq l \leq \lfloor \frac{L}{2} \rfloor.$$

Note that both of the hidden representations $\mathbf{h}^{(L)}, \mathbf{h}^{(l)} \in \mathbb{R}^{T \times d_h}$ have their length denoted as T and the hidden dimension indicated by d_h .

The hidden representations extracted from the encoder are then passed to the *aggregator*. The aggregator is designed to obtain a more compressed speech representation z that is aligned in length with the text transcription v . Consider that $v = [v_1, v_2, \dots, v_N], v_i \in \mathbb{V}$ is a text token sequence with length N , the input and output of the aggregator can be denoted as:

$$z = \text{Aggregator}(v, \mathbf{h}^{(L)}, \mathbf{h}^{(l)}), \quad \text{where } z \in \mathbb{R}^{N \times d_z}, v \in \mathbb{V}^N, \text{ and } \mathbf{h}^{(L)}, \mathbf{h}^{(l)} \in \mathbb{R}^{T \times d_h}.$$

To make the speech representation z text-aligned, we conduct a simple yet effective attention mechanism based on the three inputs. Consider that the original multi-head attention in Vaswani et al. (2017) is denoted as $\text{MultiHead}(Q, K, V)$, our first layer attention in the aggregator takes:

$$Q = \text{text transcription } v, \quad K = \text{encoder last hidden } \mathbf{h}^{(L)}, \quad V = \text{encoder shallow hidden } \mathbf{h}^{(l)}.$$

By doing so, the length of our first multi-head attention output should follow the text transcription v . Note that the query of the following layers becomes the output from the previous layer. In addition, intuitions of using the encoder’s last hidden representation as keys, and the shallow hidden representation as values can be described as follows: **1)** In Transformer-based ASR models, the last hidden states often encode rich speech-text alignment cues; sometimes the cross-attention weight matrices can even be exploited as soft word-alignment maps (Radford et al., 2023; Gandhi et al., 2023). **2)** The shallow representation has been shown to support high-quality speech reconstruction even when the quantization is applied (Du et al., 2024a;b). Based on the above observations, we design our aggregator that can use the soft attention maps obtained from the last encoder representations and the text transcriptions, to aggregate the shallow encoder representations that have been shown to be beneficial for high-end speech reconstruction.

After getting the text-aligned representation, the quantizer $\text{Quantizer}(\cdot)$ is adopted to discretize the text-aligned representation. We use the residual vector quantization (RVQ) to allow coarse-to-fine

216 quantization. Given the text-aligned speech representation z and the quantizer containing R residual
 217 vector quantization layers, we generate:
 218

$$219 \quad q, \hat{z} = \text{Quantizer}(z), \quad q = [q^{(1)}, q^{(2)}, \dots, q^{(R)}], \quad \hat{z} = \sum_{r=1}^R \hat{z}^{(r)} \quad (1)$$

221 where each $q^{(r)} \in \mathbb{C}^N$ denotes the r -th layer code sequence with code set \mathbb{C} ; and the quantized
 222 embedding \hat{z} to be the summation over each layer of the codebook vectors. Note that both of the
 223 code sequence and the quantized speech embedding \hat{z} are text-aligned, with the lengths to be N .
 224

225 **3.1.2 TASTE SPEECH DECODER**
 226

227 The speech decoder aims to perform speech reconstruction conditioned on the text token sequence
 228 and the text-aligned speech tokenization. As shown in Figure 2, the text and speech tokens are aligned
 229 in lengths and being fed into the speech decoder after weighted sum in an autoregressive manner. The
 230 speech decoder is composed of the two components: the unit decoder and the unit-to-speech vocoder.

231 The unit decoder $\text{UnitDecoder}(\cdot)$ is a Transformer-based decoder that takes the text token sequence
 232 v and the aligned speech embedding \hat{z} as condition and predicts the speech unit y for reconstruction:
 233

$$234 \quad y = \text{UnitDecoder}(\hat{z}, v). \quad (2)$$

235 Note that the additional speaker embedding is also taken as input to facilitate global speaker voice
 236 control in our spoken language models (Ju et al., 2024). After we generating the speech unit y , we
 237 use a unit-to-speech vocoder to further transform the unit into the reconstructed speech.

238 **3.1.3 TRAINING OBJECTIVE**
 239

240 Similar to other reconstruction-based speech tokens (Zhang et al., 2024; Liu et al., 2025), we derive
 241 TASTE by training it for speech resynthesis. To achieve this, we extract the speech unit y^{target} with
 242 length T' from the original speech u as the target unit for our speech tokenizer and speech decoder.
 243 Given the text transcription v , the TASTE speech embedding \hat{z} , and the unit from the original speech
 244 y^{target} as the target, the speech reconstruction through the tokenizer and the unit decoder parametrized
 245 by θ under the next prediction schema can be considered as minimizing the cross-entropy loss below:
 246

$$247 \quad \mathcal{L}_{\text{ce}}(\theta) = \frac{1}{|T'|} \sum_{t=1}^{T'} -\log p_{\theta}(y_t^{\text{target}} | \hat{z}, v; y_{<t}^{\text{target}}) \quad (3)$$

249 On the other hand, we employ the quantization loss as well to tokenize the continuous representation
 250 z extracted from the encoder-aggregator. Following prior works (Défossez et al., 2023; Zeghidour
 251 et al., 2021), given that $z^{(r)}$ is the r -th residual and $\hat{z}^{(r)}$ indicates the r -th quantized residual, the the
 252 commitment loss is defined as:
 253

$$254 \quad \mathcal{L}_{\text{rvq}}(\theta) = \sum_{r=1}^R \|z^{(r)} - \hat{z}^{(r)}\|. \quad (4)$$

255 By summation over both losses, we formulate the overall loss for training TASTE as:
 256

$$257 \quad \mathcal{L}_{\text{taste}} = \mathcal{L}_{\text{ce}} + \mathcal{L}_{\text{rvq}}. \quad (5)$$

258 Note that to allow gradient to back-propagate from the unit decoder through the tokenizer, the
 259 straight-through estimation technique is applied towards the quantization process during traning.
 260

261 **3.2 TASTE FOR SPOKEN LANGUAGE MODELING**
 262

263 Next, we describe how we conduct effective spoken language modeling with TASTE. Following
 264 previous work (Hassid et al., 2023; Nguyen et al., 2025), we perform pre-training on speech data. The
 265 text transcription of the speech data is also used for joint speech-text pre-training of our text-aligned
 266 spoken language model (TASLM). Since TASTE tokenization already aligns with the text token
 267 sequence, we can conduct a straightforward joint modeling, as illustrated in Figure 1. To demonstrate
 268 the robustness of TASTE, we perform two types of text-aligned spoken language modeling. First, we
 269 build $\text{TASLM}_{\text{token}}$ over our text-aligned speech **token** q , discussed in Section 3.2.1. Then, we show
 how we build $\text{TASLM}_{\text{emb}}$ with our text-aligned speech **embedding** \hat{z} , detailed in Section 3.2.2.

270 3.2.1 MODELING TASTE TOKEN
271

272 As our speech tokens derived from the RVQ quantizer contain R layers of codes, we employ R
273 linear heads for multi-head prediction in our $\text{TASLM}_{\text{token}}$. Namely, the $\text{TASLM}_{\text{token}}$ simultaneously
274 predicts the next text token and the corresponding R layers of speech tokens in each step. The overall
275 training objective follows the original next token prediction scheme, but with multiple predictions
276 across modalities at each step. Specifically, given the text transcription \mathbf{v} and R layers of quantized
277 RVQ codes \mathbf{q} , the multi-head next-token prediction training objective can be formulated as:
278

$$279 \mathcal{L}_{\text{token}}(\phi) = \frac{1}{|N|} \sum_{i=1}^N \left(-\log p_{\phi}^{\text{text}}(\mathbf{v}_i | \mathbf{v}_{<i}, \mathbf{q}_{<i}) + \sum_{r=1}^R -\log p_{\phi}^{(r)}(q_i^{(r)} | \mathbf{v}_{<i}, \mathbf{q}_{<i}) \right), \quad (6)$$

280 with ϕ represents the parameter of the $\text{TASLM}_{\text{token}}$, and $p^{(r)}$ is the r -th probability prediction for
281 the r -th RVQ code. As for inference, we directly sample the codes and the text simultaneously, and
282 transform the codes into the corresponding embedding for the speech decoder to generate speech.
283

284 3.2.2 MODELING TASTE EMBEDDING
285

286 Besides the token code sets, recent progress on latent modeling (Kim et al., 2024; Meng et al., 2024;
287 Sun et al., 2024; Fan et al., 2025) motivates us to conduct experiments on modeling our text-aligned
288 speech embedding. Referencing MELLE (Meng et al., 2024), we employ a linear layer that predicts
289 the mean vector μ_i and a log-magnitude variance vector $\log \sigma_i^2$, where i indicates the i -th frame
290 of the sequence. And the final predicted latent of frame i is denoted as $\mathbf{e}_i = \mu_i + \sigma_i \odot \epsilon$, where
291 $\epsilon \sim \mathcal{N}(0, I)$. Following MELLE, the straight-through estimator is applied to allow gradients to
292 back-propagate properly during training.

293 To facilitate latent prediction, we apply the regularization loss and the Kullback-Leibler (KL) diver-
294 gence loss during training, which is described as follows:

$$295 \mathcal{L}_{\text{reg}}(\psi) = \|\mathbf{e}_{\psi} - \hat{\mathbf{z}}\|_2^2, \quad \mathcal{L}_{\text{KL}} = \frac{1}{2} \sum_{i=1}^N \sum_{j=1}^{d_z} (\sigma_i[j] + (\mu_i[j] - \hat{\mathbf{z}}_i[j])^2) - 1 - \log \sigma_i^2[j], \quad (7)$$

296 where ψ indicates the parameter of $\text{TASLM}_{\text{emb}}$, and d_z is the dimension of our text-aligned embed-
297 ding $\hat{\mathbf{z}}$. The regularization loss \mathcal{L}_{reg} is adopted to predict close latent towards the target embedding
298 $\hat{\mathbf{z}}$. The KL divergence loss calculates the KL divergence between the predicted latent distribution
299 and the target distribution. Following MELLE, we select the target distribution to be $\mathcal{N}(\hat{\mathbf{z}}_i, I)$.
300 This allows simplification of \mathcal{L}_{KL} , which can then be approximated with the predicted vectors
301 μ_i, σ_i , and the target embedding $\hat{\mathbf{z}}_i$. Finally, the overall loss along with the text loss is described as:
302

$$303 \mathcal{L}_{\text{emb}}(\psi) = \lambda_{\text{reg}} \cdot \mathcal{L}_{\text{reg}} + \lambda_{\text{KL}} \cdot \mathcal{L}_{\text{KL}} + \frac{1}{|N|} \sum_{i=1}^N -\log p_{\psi}^{\text{text}}(\mathbf{v}_i | \mathbf{v}_{<i}, \hat{\mathbf{z}}_{<i}), \quad (8)$$

304 where $\lambda_{\text{reg}}, \lambda_{\text{KL}}$ to be the weighted coefficients of the two losses, respectively.
305

306 4 EXPERIMENT SETUP
307

308 **Model Configuration** For our TASTE speech tokenizer, we initialize our encoder from Whis-
309 per (Radford et al., 2023). By doing so, we can reduce computational cost between obtaining the
310 ASR transcription and extracting the TASTE tokenization with the TASTE encoder frozen during
311 training. On the other hand, we use the S3 token from Du et al. (2024a) as the target unit for speech
312 reconstruction. Since their speech tokenization facilitates additional speaker embedding, we follow
313 the same procedure to obtain one. Adding speaker embedding allows global speaker voice control,
314 which is a reasonable and useful scenario for spoken language models. The unit-to-speech vocoder
315 is comprised of a flow model (Lipman et al., 2022; Mehta et al., 2022) and a HiFiGAN. We use the
316 published pre-trained ones from Du et al. (2024a), and they are not involved in our training. For the
317 quantizer, we set the RVQ layer $R = 4$, the codebook size 512, and the codebook dimension to be
318 256. For the spoken language modeling, we follow previous work (Hassid et al., 2023) and initialize
319 our spoken language model from a text LLM. However, this introduces the vocabulary mismatch
320 problem between the ASR and LLM. We resolve this issue by using word-level TASTE tokenization
321 and embedding, which is detailed in Appendix A.4. Moreover, we conduct LoRA fine-tuning of our
322 TASLMs, with hyperparameters rank $r = 64$ and $\alpha = 128$.
323

324
 325 Table 1: **The speech tokenization evaluation results** on the *test-clean* split of LibriSpeech. The
 326 evaluation is separated into the **QUALITY** and the **SIMILARITY** assessments, as introduced in
 327 Section 5.1.1. We use gray text to indicate the worst-performing methods in each metric. Freq.
 328 indicates the number of tokens per second. All reported results already account for the effect of ASR
 329 errors whenever textual transcriptions are involved (Text-only and TASTE).

329 330 331 332 333 334 335 336 337 338 339	Method	Freq.	Bitrate	340 341 342 343 344 345 346 347 348 349 350 351 352 353 354 355 356 357 358 359 360 361 362 363 364 365 366 367 368 369 370 371 372 373 374 375 376 377			340 341 342 343 344 345 346 347 348 349 350 351 352 353 354 355 356 357 358 359 360 361 362 363 364 365 366 367 368 369 370 371 372 373 374 375 376 377			
				340 341 342 343 344 345 346 347 348 349 350 351 352 353 354 355 356 357 358 359 360 361 362 363 364 365 366 367 368 369 370 371 372 373 374 375 376 377	340 341 342 343 344 345 346 347 348 349 350 351 352 353 354 355 356 357 358 359 360 361 362 363 364 365 366 367 368 369 370 371 372 373 374 375 376 377	340 341 342 343 344 345 346 347 348 349 350 351 352 353 354 355 356 357 358 359 360 361 362 363 364 365 366 367 368 369 370 371 372 373 374 375 376 377				
Ground Truth		16k	256k	2.1%	4.09	3.84	-	-	-	76.6
Encodec ^α		75	1500	5.1%	1.58	3.26	3.46	0.94	0.63	-
		75	3000	2.6%	2.35	3.48	3.81	0.96	0.78	25.6
SpeechTokenizer ^β		50	500	5.2%	1.27	2.99	2.80	0.94	0.35	-
		50	2000	3.0%	3.56	3.60	3.65	0.97	0.80	53.9
		50	4000	2.5%	3.90	3.76	4.03	0.98	0.92	-
Mimi ^γ		12.5	1000	3.1%	3.60	3.60	3.62	0.96	0.82	67.6
S3 token ^θ (topline)		25	600	3.0%	4.18	3.90	3.30	0.96	0.82	70.2
Text-only (baseline)		~3	~50	5.9%	4.31	4.11	2.44	0.57	0.78	42.6
TASTE (ours)		~3	~150	4.4%	4.29	4.10	3.05	0.91	0.80	68.3

^α Défossez et al. (2023), ^β Zhang et al. (2024), ^γ Défossez et al. (2024), ^θ Du et al. (2024a)

Dataset We use two datasets—*Emilia* and *LibriTTS*—as our training datasets. *Emilia* (He et al., 2024) is an in-the-wild dataset where the speech is web-scaled and the transcriptions are pseudo-labeled. We use only the English subset of this multi-lingual corpus, which is about 40,000 hours. *LibriTTS* (Zen et al., 2019) is a reading-style corpus based on LibriSpeech (Panayotov et al., 2015). We use all the training splits in *LibriTTS* for training, which is approximately 600 hours of speech. In addition, the *test-clean* split in LibriSpeech is used for evaluation purposes for our TASTE tokenizer and TASLMs.

5 RESULT

We separate our experimental results into two parts. Section 5.1 discusses how TASTE strikes a good reconstruction quality while enables effective joint spoken language modeling; while Section 5.2 presents the additional results and ablation study of our joint tokenization and text-aligned SLM.

5.1 MAIN RESULTS

To demonstrate the benefits of our joint tokenization, we first evaluate the performance of TASTE on speech reconstruction; then introduce how it allows effective spoken language modeling. For simplicity, the evaluation metrics are introduced within each section.

5.1.1 TASTE FOR SPEECH RECONSTRUCTION

Evaluation We evaluate our joint tokenization on two aspects: **QUALITY** and **SIMILARITY**. For **QUALITY** assessment, we use ASR-WER, UTMOS (Saeki et al., 2022), and DNS-MOS (Reddy et al., 2021) as our metrics for evaluation. In ASR-WER, we use Hubert-Large (Hsu et al., 2021) as the ASR model to transcribe the reconstructed speech, and then calculate the word-error rate (WER) on the transcription.² UTMOS and DNS-MOS are both neural-based MOS predictors. While both evaluate the speech quality, the design purpose of DNS-MOS makes it more suitable for evaluation regarding the noise levels. For **SIMILARITY** assessment, we measure ViSQOL, duration consistency (Drtn. Con.), speaker similarity (Spkr. Sim.), and the MUSHRA human listening test score. ViSQOL (Chinen et al., 2020) is a production-ready tool that predicts speech quality via spectro-temporal image similarity comparisons. For the duration consistency, we first get the word-level alignment of the transcriptions of the original and the reconstructed speech using Montreal Forced Aligner (McAuliffe et al., 2017); then we calculate if the duration between each of the same words is matched under a preset tolerance window, which is set to 50 milliseconds. In the MUSHRA human listening test, we follow the original protocol (Series, 2014) to instruct evaluators to rate similarity and quality on a scale of 1 to 100 with reference given.

²<https://huggingface.co/facebook/hubert-large-ls960-ft>

378 **Results Analysis** Table 1 reports the results of speech reconstruction on LibriSpeech. To better
 379 understand the effectiveness of TASTE, we highlight three main observations. 1) Since our tokens are
 380 text-aligned, TASTE operates at the lowest frequency and bitrate among all tokenization methods. We
 381 estimate these dynamic values by counting the total number of tokens and accumulating the duration
 382 over the testing set. 2) Despite this extremely low bitrate, TASTE achieves on-par or even superior
 383 performance to higher-bitrate methods in the quality assessment. In particular, TASTE yields lower
 384 ASR-WER than the text-only baseline, which we attribute to speech tokens carrying paralinguistic
 385 information that improves the naturalness of reconstructed speech. 3) In terms of similarity, TASTE
 386 performs comparably to high-bitrate, fixed down-sampling methods across multiple metrics. The
 387 inferior results on ViSQL can be partly attributed to our use of a flow-based vocoder, as both
 388 TASTE and the S3 token topline exhibit weaker ViSQL performance—a phenomenon also observed
 389 in Liu et al. (2025). This degradation on ViSQL is not reflected in the MUSHRA listening test,
 390 where TASTE attains competitive perceptual quality and similarity from a human perspective. In
 391 general, TASTE significantly outperforms the text-only baseline, confirming that it carries sufficient
 392 paralinguistic information to allow high-quality speech reconstruction.

393 5.1.2 TASTE FOR SPOKEN LANGUAGE MODELING

394 TASTE is designed specifically to enable effective joint spoken language modeling (SLM). To
 395 examine its effectiveness, we train pretrained SLMs on top of TASTE following the methodology in
 396 Section 3.2. In line with prior work (Nguyen et al., 2025; Lin et al., 2024), we evaluate these models
 397 from two perspectives: speech continuation evaluation and likelihood-based evaluation.

398 **Speech Continuation Evaluation** First, each pretrained SLM is conditioned on 3-second speech
 399 segments from LibriSpeech *test-clean* to generate speech continuations under their own decoding
 400 schemes, following Hassid et al. (2023); Lin et al. (2024). The generated continuations are then
 401 evaluated along two main aspects: *semantic coherence* and *speech naturalness*. For the semantic
 402 aspect, we transcribe the continuations using ASR and ask GPT-4o to assign MOS scores based on
 403 their coherence. For the speech naturalness aspect, we compute UTMOS as an objective score of
 404 speech quality. In addition, human evaluators provide an overall MOS score that jointly considers
 405 both coherence and naturalness. The detailed instructions given to GPT-4o and human evaluators are
 406 provided in Appendix A.3.2.

407 **Likelihood-Based Evaluation** Following previous work (Hassid et al., 2023; Nguyen et al., 2025;
 408 Lin et al., 2024), we also evaluate the SLMs through likelihood-based benchmarks, where the
 409 accuracy score is based on whether the pretrained SLM chooses the correct continuation from the
 410 two given speech utterances based on its output likelihoods. We adopt two established benchmarks
 411 SALMON (Maimon et al., 2024) and spoken StoryCloze (Hassid et al., 2023; Mostafazadeh et al.,
 412 2024).

413 **Table 2: Pretrained SLM speech continuation and likelihood-based next-speech selection results.**
 414 The superscripts at the bottom of the table indicate the base models used by each SLM, indicated by
 415 superscripts. Cascade models refer to the pipeline with ASR (Radford et al., 2023), text continuation
 416 by LMs (Touvron et al., 2023), and TTS (Du et al., 2024a). This allow us to evaluate SLMs with
 417 cascade models in continuation perspective.

421 Method	Finetuned / base parameters	CONTINUATION			LIKELIHOOD			Overall
		GPT-4o	UTMOS	Human	SALMON	StoryCloze		
<i>Cascade</i>								
Cascade (LLaMA3.2-1B ^α)	-	3.15	4.25	4.00	-	-	-	-
Cascade (LLaMA2-7B ^β)	-	3.43	4.25	3.98	-	-	-	-
<i>Spoken LMs</i>								
TWIST 1.3B (Hassid et al., 2023)	1.3B / 1.3B ^θ	1.48	3.25	1.95	62.5	61.5	62.0	
TWIST 7B (Hassid et al., 2023)	7B / 7B ^γ	1.44	3.27	2.04	63.4	64.7	64.1	
Spirit LM (Nguyen et al., 2025)	7B / 7B ^β	2.79	3.41	2.38	59.1	72.0	65.6	
Spirit LM Expr. (Nguyen et al., 2025)	7B / 7B ^β	1.90	3.40	2.41	69.0	66.2	67.6	
Baseline (S3 token)	45M / 1.3B ^α	1.37	4.04	2.84	50.2	58.7	54.5	
TASLM 1B (token)	45M / 1.3B ^α	3.08	4.07	3.93	60.8	76.5	68.7	
TASLM 1B (embed.)	45M / 1.3B ^α	3.16	4.22	4.16	57.7	76.7	67.2	

431 Base models: ^αLLaMA3.2-1B, ^βLLaMA2-7B, ^γLLaMA-7B, ^θOPT-1.3B

2016), which covers the acoustic aspect and the semantic aspect, respectively. Since both benchmarks contain multiple tasks, we report the average accuracy across these tasks within each benchmark for simplicity. The detailed results are in Appendix A.1.5 for the interested readers. We also report the mean of the SALMON and StoryCloze as an overall assessment for both aspects.

Results Analysis The results of TASLM compared to other pre-trained SLMs are shown in Table 2, and three main advantages can be observed. **1)** Compared to other pretrained SLMs, TASLM achieves substantially better performance on speech continuation across both human and machine evaluations, while also performing competitively on the likelihood-based benchmarks. Notably, this is achieved with only LoRA finetuning on a relatively small 1.3B base language model, illustrating the effectiveness of TASTE for joint modeling. **2)** Compared to cascade models with the same base LM, our TASLM_{emb} achieves comparable scores on GPT-4o but higher human MOS. This indicates that its generated speech is more natural than cascade systems that rely solely on TTS during continuation. TASLM is the only SLM that not only maintains but even surpasses the performance of its corresponding text-based model, highlighting the importance of speech token modeling. **3)** Directly using the S3 token for joint modeling following Xie & Wu (2024a) yields poor performance across *all* aspects, even though it surpasses TASTE in speech reconstruction. This shows that while reconstruction quality is critical, it is not the sole consideration in tokenization for spoken language modeling. Taken together, these results highlight the central contribution of TASTE: **building a joint tokenization that facilitates more effective joint spoken language modeling.**

5.2 ADDITIONAL RESULTS

5.2.1 TASTE FOR TEXT-ALIGNED SPEECH EDITING

Beyond the main results presented above, we report several intriguing observations that further showcase the versatility of TASTE. The first is that TASTE naturally enables *text-aligned speech editing*, as illustrated in Figure 3. Suppose we have two utterances with the same transcript but different paralinguistic characteristics. By exchanging their TASTE token sequences word by word, we ask whether the associated paralinguistic traits are transferred as well. To make the effect clear, we select utterances that differ mainly in speaking rate and examine duration changes using MFA (McAuliffe et al., 2017). As illustrated in Figure 3, swapping tokens at specific word positions causes the corresponding words to exhibit clear duration shifts, while untouched words preserve their original timing—evidence that TASTE enables precise, text-aligned manipulation. This observation also echoes our design principle introduced in Section 1: a speech token should avoid redundantly encoding text content and instead concentrate on conveying paralinguistic information. Additional examples targeting other paralinguistic dimensions are provided on our demo page.

5.2.2 TASLM FOR SPOKEN QUESTION ANSWERING

Next, we intriguingly find out that our TASLM exhibits spoken QA ability under few-shot scenario (Brown et al., 2020). We are the only pretrained SLM in Table 2 that exhibits this capability. As

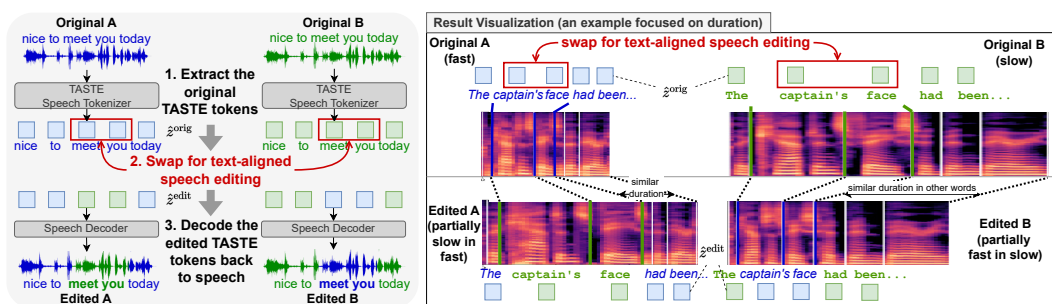


Figure 3: **An illustration of TASTE for text-aligned speech editing.** On the left shows the process of our text-aligned speech editing. We first extract the TASTE tokens; swap the tokens partially; and then decode the edited TASTE tokens into edited speech. On the right shows an example visualization. Only the durations of the words with exchanged TASTE tokens show significant difference.

Table 3: **Evaluation of spoken question answering.** Performance across modalities is compared row-wise, where T is text and S denotes speech.

Method	Mode	Web Q.	LLaMA-Q.
Mini-Omni 0.5B($T \rightarrow T$)	T	21.3	39.0
Mini-Omni 0.5B	T+S	4.5	11.6
Helium 7B (text)	T	32.3	75.0
Moshi 7B	T+S	26.6	62.3
LLaMA3.1-8B-Instruct	T	60.4	71.7
Llama-Omni-8B	T+S	35.5	67.3
LLaMA3.2-1B †	T	24.0	51.0
TASLM 1B (embed.) †	T+S	27.1	57.6

[†] We apply few-shot learning to facilitate question answering.

Table 4: **Ablation study on the effects of each module in TASTE speech tokenizer.** Enc. is *encoder*, Agg. is *aggregator*, and Quan. is *quantizer*. *: top-5 accuracy.

Modules	Freq.	S3 token Acc.*
Enc.	50Hz	0.98
Enc. + Agg.	~3Hz	0.88
Enc. + Agg. + Quan.	~3Hz	0.76
Enc. (last)	50Hz	0.84
Enc. + Agg. (last)	~3Hz	0.78
Text-only	~3Hz	0.65

a result, we compare it against other instruction-finetuned joint SLMs in Table 3 to better understand the performance. We use two spoken question answering benchmarks, Web Questions (Berant et al., 2013) and LLaMA-Questions (Nachmani et al., 2024), following Défossez et al. (2024). We report the accuracy of answer containment. To more comprehensively assess the impact of adding speech, we also report the performance of each system’s underlying base text LLM. Notably, TASLM is the only approach that preserves its base text LLM’s performance. We attribute this to TASTE’s joint tokenization strategy. Specifically, we employ a straightforward one-to-one mapping between text and speech tokens, which enables simple and effective joint modeling.

5.2.3 ABLATION STUDY ON TASTE SPEECH TOKENIZER

We run an ablation on TASTE speech tokenizer and use S3 token top-5 reconstruction accuracy as a proxy for information retention. Table 4 first covers the module-wise ablations of our *encoder*, *aggregator*, and *quantizer*. The *aggregator* sharply reduces token rate with only a small drop in accuracy. Adding the *quantizer* lowers accuracy further, but performance is still well above the text-only baseline. Secondly, we show that using only the *last* hidden state $\mathbf{h}^{(L)}$ performs worse than using the *shallow* hidden states $\mathbf{h}^{(l)}$ (as values for the aggregator), confirming our design choice.

6 CONCLUSION

In this work, we propose Text-Aligned Speech Tokenization and Embedding (TASTE), to facilitate joint text-speech spoken language modeling. By aggregating proper encoder representation through the specialized cross-attention mechanism and taking the ASR model as initialization, we make the speech tokenization text-aligned in an end-to-end manner with no explicit word alignment required. With our text-aligned speech tokenization and embedding, joint text-speech modeling becomes straightforward and effective. We conduct extensive experiments demonstrating the benefits of developing a joint tokenization tailored for spoken language modeling. We anticipate that these findings encourage further research on more effective joint tokenization for generative modeling.

Limitation Several limitations of our current work suggest promising avenues for future development. First, while our pretrained spoken language model generates high-quality audio continuations, it lacks mechanisms for turn-taking and instruction following; developing a dialogue system is a practical next step. Second, TASTE has so far been evaluated on English; confirming its generalizability across other languages remains future work. Third, our tokenization method is tailored for joint SLMs, and its applicability to other generative tasks remains underexplored. Fourth, our pipeline currently focuses on single-speaker speech with lexical content and does not explicitly handle multi-speaker, overlapping, or non-lexical events (*e.g.*, laughter, coughing). Future work could support these capabilities by incorporating target speech extraction (Zmolikova et al., 2023) and non-lexical event tags. Finally, system latency and streaming performance are yet to be optimized for real-time applications. Overall, none of these limitations is a fundamental barrier; rather, they are natural extensions and research targets that will further enhance the versatility of TASTE framework.

540 **Ethics Statement** TASTE enables the efficient development of spoken language models. It lowers
 541 the barrier to building speech systems and improves the accessibility and convenience of hu-
 542 man-computer interaction. At the same time, it raises security concerns: systems built with TASTE
 543 can more easily mimic a person’s voice and synthesize convincing personalized speech. Moreover,
 544 TASTE’s text-aligned speech editing makes voice manipulation straightforward. Overall, TASTE
 545 offers clear utility for beneficial applications, but responsible deployment—paired with consent,
 546 provenance, and anti-abuse safeguards—is essential to mitigate misuse risks. On the other hand, this
 547 study includes human evaluations in the form of subjective listening tests. Annotators were recruited
 548 from Amazon Mechanical Turk and compensated fairly according to the platform’s recommended
 549 rates. All participants provided informed consent, and no personal information has been collected.
 550 The audio material used in the evaluation does not contain sensitive content. The study adheres to the
 551 ethical standards commonly adopted in speech perception research.
 552

553 REFERENCES

554 Md Mubtasim Ahasan, Md Fahim, Tasnim Mohiuddin, Akmmahbubur Rahman, Aman Chadha, Tariq
 555 Iqbal, M Ashraful Amin, Md Mofijul Islam, and Amin Ahsan Ali. DM-codec: Distilling multi-
 556 modal representations for speech tokenization. In *Findings of the Association for Computational
 557 Linguistics: EMNLP 2025*, 2025.

558 Siddhant Arora, Kai-Wei Chang, Chung-Ming Chien, Yifan Peng, Haibin Wu, Yossi Adi, Emmanuel
 559 Dupoux, Hung-Yi Lee, Karen Livescu, and Shinji Watanabe. On the landscape of spoken language
 560 models: A comprehensive survey. *arXiv preprint arXiv:2504.08528*, 2025.

561 Alexei Baevski, Yuhao Zhou, Abdelrahman Mohamed, and Michael Auli. wav2vec 2.0: A frame-
 562 work for self-supervised learning of speech representations. In *Advances in Neural Information
 563 Processing Systems*, 2020.

564 Jonathan Berant, Andrew Chou, Roy Frostig, and Percy Liang. Semantic parsing on freebase from
 565 question-answer pairs. In *Proceedings of the 2013 conference on empirical methods in natural
 566 language processing*, 2013.

567 Tom Brown, Benjamin Mann, Nick Ryder, Melanie Subbiah, Jared D Kaplan, Prafulla Dhariwal,
 568 Arvind Neelakantan, Pranav Shyam, Girish Sastry, Amanda Askell, et al. Language models are
 569 few-shot learners. *Advances in neural information processing systems*, 2020.

570 Li-Wei Chen and Alexander Rudnicky. Fine-grained style control in transformer-based text-to-speech
 571 synthesis. In *ICASSP 2022-2022 IEEE International Conference on Acoustics, Speech and Signal
 572 Processing (ICASSP)*, 2022.

573 Sanyuan Chen, Shujie Liu, Long Zhou, Yanqing Liu, Xu Tan, Jinyu Li, Sheng Zhao, Yao Qian, and
 574 Furu Wei. Vall-e 2: Neural codec language models are human parity zero-shot text to speech
 575 synthesizers. *arXiv preprint arXiv:2406.05370*, 2024.

576 Cheng-Han Chiang and Hung-yi Lee. Can large language models be an alternative to human
 577 evaluations? In *Proceedings of the 61st Annual Meeting of the Association for Computational
 578 Linguistics (Volume 1: Long Papers)*, 2023.

579 Michael Chinen, Felicia SC Lim, Jan Skoglund, Nikita Gureev, Feargus O’Gorman, and Andrew
 580 Hines. Visql v3: An open source production ready objective speech and audio metric. In *2020
 581 twelfth international conference on quality of multimedia experience (QoMEX)*, 2020.

582 Alexandre Défossez, Jade Copet, Gabriel Synnaeve, and Yossi Adi. High fidelity neural audio
 583 compression. *Transactions on Machine Learning Research*, 2023.

584 Alexandre Défossez, Laurent Mazaré, Manu Orsini, Amélie Royer, Patrick Pérez, Hervé Jégou,
 585 Edouard Grave, and Neil Zeghidour. Moshi: a speech-text foundation model for real-time dialogue.
 586 *arXiv preprint arXiv:2410.00037*, 2024.

587 Zhihao Du, Qian Chen, Shiliang Zhang, Kai Hu, Heng Lu, Yexin Yang, Hangrui Hu, Siqi Zheng,
 588 Yue Gu, Ziyang Ma, et al. Cosyvoice: A scalable multilingual zero-shot text-to-speech synthesizer
 589 based on supervised semantic tokens. *arXiv preprint arXiv:2407.05407*, 2024a.

594 Zhihao Du, Yuxuan Wang, Qian Chen, Xian Shi, Xiang Lv, Tianyu Zhao, Zhifu Gao, Yexin Yang,
 595 Changfeng Gao, Hui Wang, et al. Cosyvoice 2: Scalable streaming speech synthesis with large
 596 language models. *CoRR*, 2024b.

597 Lijie Fan, Luming Tang, Siyang Qin, Tianhong Li, Xuan Yang, Siyuan Qiao, Andreas Steiner, Chen
 598 Sun, Yuanzhen Li, Tao Zhu, et al. Unified autoregressive visual generation and understanding with
 599 continuous tokens. *arXiv preprint arXiv:2503.13436*, 2025.

600 Qingkai Fang, Shoutao Guo, Yan Zhou, Zhengrui Ma, Shaolei Zhang, and Yang Feng. Llama-omni:
 601 Seamless speech interaction with large language models. *CoRR*, 2024.

602 Sanchit Gandhi, Patrick von Platen, and Alexander M Rush. Distil-whisper: Robust knowledge
 603 distillation via large-scale pseudo labelling. *arXiv preprint arXiv:2311.00430*, 2023.

604 Alex Graves. Sequence transduction with recurrent neural networks. *arXiv preprint arXiv:1211.3711*,
 605 2012.

606 Michael Hassid, Tal Remez, Tu Anh Nguyen, Itai Gat, Alexis Conneau, Felix Kreuk, Jade Copet,
 607 Alexandre Defossez, Gabriel Synnaeve, Emmanuel Dupoux, et al. Textually pretrained speech
 608 language models. *Advances in Neural Information Processing Systems*, 2023.

609 Haorui He, Zengqiang Shang, Chaoren Wang, Xuyuan Li, Yicheng Gu, Hua Hua, Liwei Liu, Chen
 610 Yang, Jiaqi Li, Peiyang Shi, et al. Emilia: An extensive, multilingual, and diverse speech dataset
 611 for large-scale speech generation. In *2024 IEEE Spoken Language Technology Workshop (SLT)*,
 2024.

612 Harold Hotelling. Relations between two sets of variates. In *Breakthroughs in statistics: methodology*
 613 and distribution. Springer, 1992.

614 Pin-Lun Hsu, Yun Dai, Vignesh Kothapalli, Qingquan Song, Shao Tang, Siyu Zhu, Steven Shimizu,
 615 Shivam Sahni, Haowen Ning, and Yanning Chen. Liger kernel: Efficient triton kernels for llm
 616 training. *arXiv preprint arXiv:2410.10989*, 2024.

617 Wei-Ning Hsu, Benjamin Bolte, Yao-Hung Hubert Tsai, Kushal Lakhota, Ruslan Salakhutdinov,
 618 and Abdelrahman Mohamed. Hubert: Self-supervised speech representation learning by masked
 619 prediction of hidden units. *IEEE/ACM Transactions on Audio, Speech, and Language Processing*,
 2021.

620 Edward J Hu, Yelong Shen, Phillip Wallis, Zeyuan Allen-Zhu, Yuanzhi Li, Shean Wang, Lu Wang,
 621 and Weizhu Chen. Lora: Low-rank adaptation of large language models. *arXiv preprint*
 622 *arXiv:2106.09685*, 2021.

623 Zeqian Ju, Yuancheng Wang, Kai Shen, Xu Tan, Detai Xin, Dongchao Yang, Yanqing Liu, Yichong
 624 Leng, Kaitao Song, Siliang Tang, et al. Naturalspeech 3: Zero-shot speech synthesis with factorized
 625 codec and diffusion models. *International Conference on Machine Learning*, 2024.

626 Jaehyeon Kim, Keon Lee, Seungjun Chung, and Jaewoong Cho. Clam-tts: Improving neural codec
 627 language model for zero-shot text-to-speech. *ICLR*, 2024.

628 Diederik P Kingma. Adam: A method for stochastic optimization. In *International Conference on*
 629 *Learning Representations*, 2015.

630 Rithesh Kumar, Prem Seetharaman, Alejandro Luebs, Ishaan Kumar, and Kundan Kumar. High-
 631 fidelity audio compression with improved rvqgan. *Advances in Neural Information Processing*
 632 *Systems*, 2023.

633 Kushal Lakhota, Eugene Kharitonov, Wei-Ning Hsu, Yossi Adi, Adam Polyak, Benjamin Bolte,
 634 Tu-Anh Nguyen, Jade Copet, Alexei Baevski, Abdelrahman Mohamed, et al. On generative spoken
 635 language modeling from raw audio. *Transactions of the Association for Computational Linguistics*,
 2021.

636 Yadong Li, Jun Liu, Tao Zhang, Song Chen, Tianpeng Li, Zehuan Li, Lijun Liu, Lingfeng Ming, Gu-
 637 osheng Dong, Da Pan, et al. Baichuan-omni-1.5 technical report. *arXiv preprint arXiv:2501.15368*,
 2025.

648 Guan-Ting Lin, Prashanth Gurunath Shivakumar, Aditya Gourav, Yile Gu, Ankur Gandhe, Hung-yi
 649 Lee, and Ivan Bulyko. Align-slm: Textless spoken language models with reinforcement learning
 650 from ai feedback. *arXiv preprint arXiv:2411.01834*, 2024.

651

652 Yaron Lipman, Ricky TQ Chen, Heli Ben-Hamu, Maximilian Nickel, and Matt Le. Flow matching
 653 for generative modeling. *The Eleventh International Conference on Learning Representations*,
 654 2022.

655 Alexander H Liu, Sang-gil Lee, Chao-Han Huck Yang, Yuan Gong, Yu-Chiang Frank Wang, James R
 656 Glass, Rafael Valle, and Bryan Catanzaro. Uniwav: Towards unified pre-training for speech
 657 representation learning and generation. *The Thirteenth International Conference on Learning
 658 Representations*, 2025.

659

660 Ilya Loshchilov and Frank Hutter. Decoupled weight decay regularization. In *International Conference
 661 on Learning Representations*, 2019.

662 Gallil Maimon, Amit Roth, and Yossi Adi. Salmon: A suite for acoustic language model evaluation.
 663 *arXiv preprint arXiv:2409.07437*, 2024.

664

665 Michael McAuliffe, Michaela Socolof, Sarah Mihuc, Michael Wagner, and Morgan Sonderegger.
 666 Montreal forced aligner: Trainable text-speech alignment using kaldi. In *Interspeech 2017*, 2017.

667

668 Shivam Mehta, Ambika Kirkland, Harm Lameris, Jonas Beskow, Éva Székely, and Gustav Eje Henter.
 669 Overflow: Putting flows on top of neural transducers for better tts. *Interspeech 2023*, 2022.

670

671 Lingwei Meng, Long Zhou, Shujie Liu, Sanyuan Chen, Bing Han, Shujie Hu, Yanqing Liu, Jinyu Li,
 672 Sheng Zhao, Xixin Wu, et al. Autoregressive speech synthesis without vector quantization. *CoRR*,
 2024.

673

674 Nasrin Mostafazadeh, Nathanael Chambers, Xiaodong He, Devi Parikh, Dhruv Batra, Lucy Van-
 675 derwende, Pushmeet Kohli, and James Allen. A corpus and evaluation framework for deeper
 676 understanding of commonsense stories. *Proceedings of NAACL-HLT*, 2016.

677

678 Eliya Nachmani, Alon Levkovich, Roy Hirsch, Julian Salazar, Chulayuth Asawaroengchai, Soroosh
 679 Mariooryad, Ehud Rivlin, RJ Skerry-Ryan, and Michelle Tadmor Ramanovich. Spoken question
 680 answering and speech continuation using spectrogram-powered llm. In *The Twelfth International
 Conference on Learning Representations*, 2024.

681

682 Tu Anh Nguyen, Eugene Kharitonov, Jade Copet, Yossi Adi, Wei-Ning Hsu, Ali Elkahky, Paden
 683 Tomasello, Robin Algayres, Benoît Sagot, Abdelrahman Mohamed, et al. Generative spoken
 684 dialogue language modeling. *Transactions of the Association for Computational Linguistics*, 2023.

685

686 Tu Anh Nguyen, Benjamin Muller, Bokai Yu, Marta R Costa-Jussa, Maha Elbayad, Sravya Popuri,
 687 Christophe Ropers, Paul-Ambroise Duquenne, Robin Algayres, Ruslan Mavlyutov, et al. Spirit-lm:
 688 Interleaved spoken and written language model. *Transactions of the Association for Computational
 689 Linguistics*, 2025.

690

691 Vassil Panayotov, Guoguo Chen, Daniel Povey, and Sanjeev Khudanpur. Librispeech: An asr corpus
 692 based on public domain audio books. In *2015 IEEE International Conference on Acoustics, Speech
 693 and Signal Processing (ICASSP)*, 2015.

694

695 Ankita Pasad, Ju-Chieh Chou, and Karen Livescu. Layer-wise analysis of a self-supervised speech
 696 representation model. In *2021 IEEE Automatic Speech Recognition and Understanding Workshop
 697 (ASRU)*, 2021.

698

699 Alec Radford, Jong Wook Kim, Tao Xu, Greg Brockman, Christine McLeavey, and Ilya Sutskever.
 700 Robust speech recognition via large-scale weak supervision. In *International conference on
 701 machine learning*, 2023.

702

703 Jeff Rasley, Samyam Rajbhandari, Olatunji Ruwase, and Yuxiong He. Deepspeed: System optimiza-
 704 tions enable training deep learning models with over 100 billion parameters. In *Proceedings of the
 705 26th ACM SIGKDD international conference on knowledge discovery and data mining*, 2020.

702 Chandan KA Reddy, Vishak Gopal, and Ross Cutler. Dnsmos: A non-intrusive perceptual objective
 703 speech quality metric to evaluate noise suppressors. In *ICASSP 2021-2021 IEEE International*
 704 *Conference on Acoustics, Speech and Signal Processing (ICASSP)*, 2021.

705 Takaaki Saeki, Detai Xin, Wataru Nakata, Tomoki Koriyama, Shinnosuke Takamichi, and Hiroshi
 706 Saruwatari. Utmos: Utokyo-sarulab system for voicemos challenge 2022. *Interspeech 2022*, 2022.

708 Monica Sekoyan, Nithin Rao Koluguri, Nune Tadevosyan, Piotr Zelasko, Travis Bartley, Nick Karpov,
 709 Jagadeesh Balam, and Boris Ginsburg. Canary-1b-v2 & parakeet-tdt-0.6 b-v3: Efficient and
 710 high-performance models for multilingual asr and ast. *arXiv preprint arXiv:2509.14128*, 2025.

711 B Series. Method for the subjective assessment of intermediate quality level of audio systems.
 712 *International Telecommunication Union Radiocommunication Assembly*, 2014.

713 Hubert Siuzdak, Florian Grötschla, and Luca A Lanzendörfer. Snac: Multi-scale neural audio codec.
 714 *Audio Imagination: NeurIPS 2024 Workshop AI-Driven Speech, Music, and Sound Generation*,
 715 2024.

717 Yutao Sun, Hangbo Bao, Wenhui Wang, Zhiliang Peng, Li Dong, Shaohan Huang, Jianyong Wang,
 718 and Furu Wei. Multimodal latent language modeling with next-token diffusion. *arXiv preprint*
 719 *arXiv:2412.08635*, 2024.

720 Hugo Touvron, Thibaut Lavril, Gautier Izacard, Xavier Martinet, Marie-Anne Lachaux, Timothée
 721 Lacroix, Baptiste Rozière, Naman Goyal, Eric Hambro, Faisal Azhar, et al. Llama: Open and
 722 efficient foundation language models. *arXiv preprint arXiv:2302.13971*, 2023.

723 Ashish Vaswani, Noam Shazeer, Niki Parmar, Jakob Uszkoreit, Llion Jones, Aidan N Gomez, Łukasz
 724 Kaiser, and Illia Polosukhin. Attention is all you need. *Advances in neural information processing*
 725 *systems*, 2017.

727 Chengyi Wang, Sanyuan Chen, Yu Wu, Ziqiang Zhang, Long Zhou, Shujie Liu, Zhuo Chen, Yanqing
 728 Liu, Huaming Wang, Jinyu Li, et al. Neural codec language models are zero-shot text to speech
 729 synthesizers. *arXiv preprint arXiv:2301.02111*, 2023.

730 Zhifei Xie and Changqiao Wu. Mini-omni: Language models can hear, talk while thinking in
 731 streaming. *arXiv preprint arXiv:2408.16725*, 2024a.

732 Zhifei Xie and Changqiao Wu. Mini-omni2: Towards open-source gpt-4o with vision, speech and
 733 duplex capabilities. *arXiv preprint arXiv:2410.11190*, 2024b.

735 Detai Xin, Xu Tan, Kai Shen, Zeqian Ju, Dongchao Yang, Yuancheng Wang, Shinnosuke Takamichi,
 736 Hiroshi Saruwatari, Shujie Liu, Jinyu Li, et al. Rall-e: Robust codec language modeling with
 737 chain-of-thought prompting for text-to-speech synthesis. *arXiv preprint arXiv:2404.03204*, 2024a.

738 Detai Xin, Xu Tan, Shinnosuke Takamichi, and Hiroshi Saruwatari. Bigcodec: Pushing the limits of
 739 low-bitrate neural speech codec. *arXiv preprint arXiv:2409.05377*, 2024b.

740 Hainan Xu, Fei Jia, Somshubra Majumdar, He Huang, Shinji Watanabe, and Boris Ginsburg. Efficient
 741 sequence transduction by jointly predicting tokens and durations. In *International Conference on*
 742 *Machine Learning*, 2023.

743 Neil Zeghidour, Alejandro Luebs, Ahmed Omran, Jan Skoglund, and Marco Tagliasacchi. Sound-
 744 stream: An end-to-end neural audio codec. *IEEE/ACM Transactions on Audio, Speech, and*
 745 *Language Processing*, 2021.

747 Heiga Zen, Viet Dang, Rob Clark, Yu Zhang, Ron J Weiss, Ye Jia, Zhifeng Chen, and Yonghui Wu.
 748 Libritts: A corpus derived from librispeech for text-to-speech. *Interspeech 2019*, 2019.

749 Aohan Zeng, Zhengxiao Du, Mingdao Liu, Kedong Wang, Shengmin Jiang, Lei Zhao, Yuxiao Dong,
 750 and Jie Tang. Glm-4-voice: Towards intelligent and human-like end-to-end spoken chatbot. *arXiv*
 751 *preprint arXiv:2412.02612*, 2024.

752 Xin Zhang, Dong Zhang, Shimin Li, Yaqian Zhou, and Xipeng Qiu. Speechtokenizer: Unified speech
 753 tokenizer for speech large language models. *ICLR*, 2024.

755 Katerina Zmolikova, Marc Delcroix, Tsubasa Ochiai, Keisuke Kinoshita, Jan Černocký, and Dong
 756 Yu. Neural target speech extraction: An overview. *IEEE Signal Processing Magazine*, 2023.

756
757
758
759
760
761
762
763
764
765
766
767
768
769
770
771
772
773
774
775
776
777
778
779
780
781
782
783
784
785
786
787
788
789
790
791
792
793
794
795
796
797
798
799
800
801
802
803
804
805
806
807
808
809
Table 5: The ablation study on how the ASR affects the performance of our TASTE tokenizer regarding speech reconstruction. GT: ground-truth transcription.

Method	WER	UTMOS	DNS-MOS	ViSQOL	Drtn. Con.	Spkr. Sim.
TASTE (w/ ASR)	4.4%	4.29	4.10	3.05	0.91	0.80
TASTE (w/ GT)	4.6%	4.24	4.08	3.06	0.91	0.81

756
757
758
759
760
761
762
763
764
765
766
767
768
769
770
771
772
773
774
775
776
777
778
779
780
781
782
783
784
785
786
787
788
789
790
791
792
793
794
795
796
797
798
799
800
801
802
803
804
805
806
807
808
809
Table 6: The ablation study on how the ASR affects our SLM on spoken QA.

Methods	Web-Q	LLaMA-Q
TASLM (w/ ASR)	27.1	57.6
TASLM (w/ GT)	28.0	57.7

762
763
764
765
766
767
768
769
770
771
772
773
774
775
776
777
778
779
780
781
782
783
784
785
786
787
788
789
790
791
792
793
794
795
796
797
798
799
800
762
763
764
765
766
767
768
769
770
771
772
773
774
775
776
777
778
779
780
781
782
783
784
785
786
787
788
789
790
791
792
793
794
795
796
797
798
799
800
Table 7: The ablation study on using a different ASR model regarding the SLM continuation semantic evaluation. Overall, we do not observe significant *relative* performance difference.

Evaluation Models	TWIST 1.3B	TWIST 7B	Spirit LM	Spirit LM Expr.	S3 token	TASLM (token)	TASLM (embed.)
Whisper + GPT-4o	1.48	1.44	2.79	1.90	1.37	3.08	3.16
nvidia-parakeet + GPT-4o	1.38	1.49	2.76	2.06	1.42	3.20	3.37

A APPENDIX

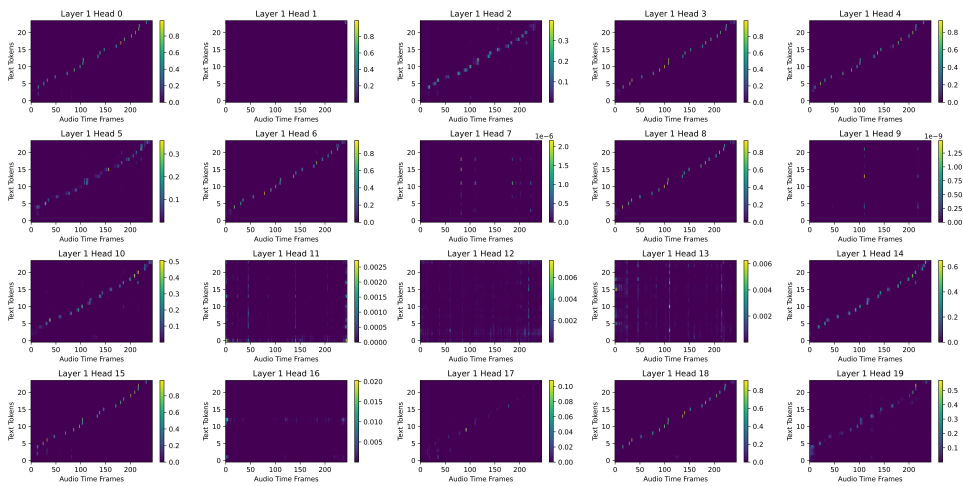
A.1 SUPPLEMENTARY RESULTS

A.1.1 ABLATION STUDY ON THE EFFECT OF ASR

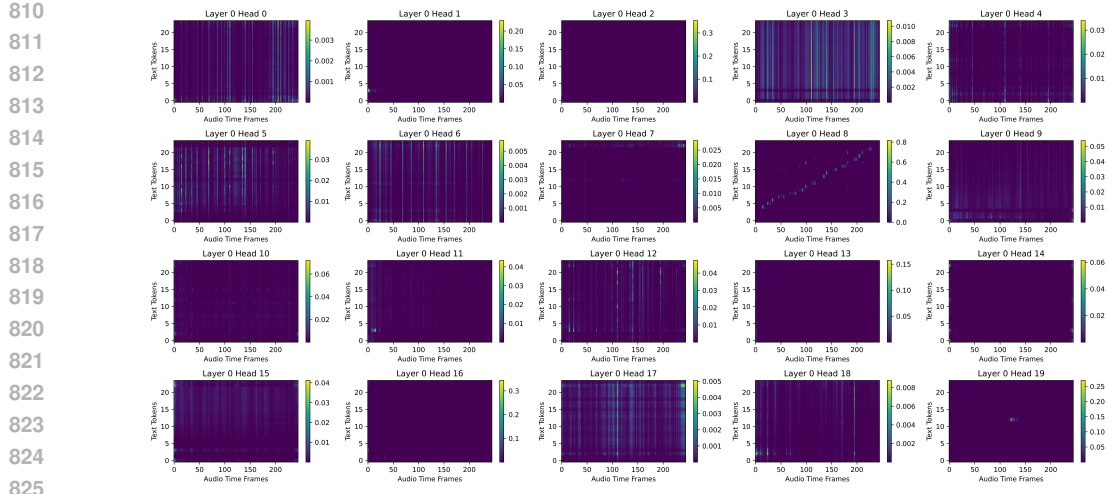
Because our tokenization, SLM, as well as the evaluation using GPT-4o all rely on an ASR system to extract text transcriptions, we conduct several ablation studies to assess the impact of ASR on performance. **1)** In Table 5 and Table 6, we study how the ASR affects the performance of our TASTE tokenizer on speech reconstruction and TASLM on spoken question answering. Our results indicate that on both the tokenization and the SLM stages, the performance drop introduced by the ASR errors are almost negligible, primarily attributed to the robustness of recent ASR systems. Note that we do not use any ground-truth transcriptions in the previous experiments in the main text. **2)** We study how substituting the ASR used to produce transcripts before GPT-4o’s semantic-coherence evaluation affects the reported scores. As shown in Table 7, we use another ASR model named nvidia-parakeet (Sekoyan et al., 2025), which employs an RNN-T (Graves, 2012; Xu et al., 2023) backbone. The results indicate that there is no significant relative performance difference between using Whisper and nvidia-parakeet ASR systems. TASLMs achieve much better results in both evaluation setups compared to the other pretrained SLMs.

A.1.2 AGGREGATOR CROSS ATTENTION VISUALIZATION

To understand whether the aggregator has learned the text-speech aligned pattern, we visualize its cross attention map across all the layers and heads in Figure 4 and Figure 5.



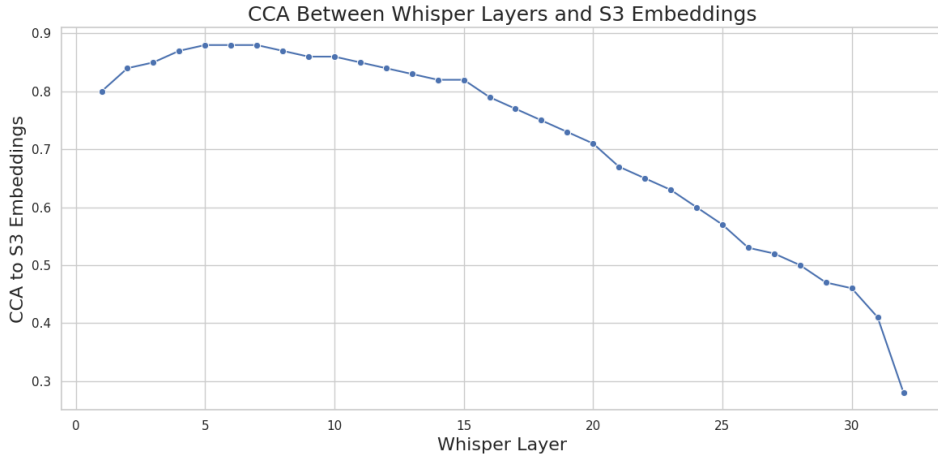
801
802
803
804
805
806
807
808
809
Figure 4: The cross attention map of the last layer in our aggregator. As illustrated, a lot of heads clearly demonstrate the text-speech aligned behavior.



826 **Figure 5: The cross attention map of the first layer in our aggregator.** As illustrated, the behavior
827 is quite different from the last layer in Figure 4. We observe some special heads: Head 8th shows
828 clear alignment; while head 19th lights up at the silence part.

831 A.1.3 DISCUSSION ON THE SELECTION OF SHALLOW HIDDEN LAYER

833 In Section 3.1.1, we propose using the shallow hidden representation from Whisper encoder as the
834 key in our specialized cross attention, as it carries rich acoustic information. In practice, we select
835 $l = 6$. In Table 4, this allows us to achieve a near-optimal reconstruction accuracy on the target S3
836 unit. To further justify this selection, we follow the analysis methodology of Pasad et al. (2021) and
837 compute the Canonical Correlation Analysis (CCA; Hotelling (1992)) between each Whisper encoder
838 layer and the target S3 unit embeddings. The resulting similarity curve is shown in Figure 6. The
839 correlations peak at the 4-th to 8-th layers, indicating that these shallow layers encode representations
840 most aligned with the S3 targets—supporting our design choice of using a shallow hidden state.
841 Importantly, Table 4 also shows that while the choice of the shallow layer affects the attainable upper
842 bound, it does not impose a strict limitation on our method: even using the final encoder layer, whose
843 correlation to S3 is much lower, still yields reconstruction quality better than the text-only baseline.



864 **Figure 6: Canonical Correlation Analysis (CCA) between each Whisper encoder layer and the**
865 **S3 target embeddings.** Layers 4–8 exhibit the highest correlation with the S3 units, indicating that
866 shallow representations contain the most target-relevant acoustic information.

864
 865 **Table 8: The tokenizer robustness ablation study.** We apply four different level of noise, with
 866 signal-to-noise ratio (SNR) ranging from 20dB (almost clean) to 5dB (very noisy). Our method
 867 substantially achieves good reconstruction quality across all noise levels.

Method	Bitrate	SNR=20dB (clean)			SNR=15dB			SNR=10dB			SNR=5dB (noisy)		
		WER ↓	Sim. ↑	Rank	WER ↓	Sim. ↑	Rank	WER ↓	Sim. ↑	Rank	WER ↓	Sim. ↑	Rank
Ground Truth	256k	2.3%	-	-	2.5%	-	-	3.6%	-	-	9.2%	-	-
DAC ^α	500	93.7%	0.193	13	97.7%	0.201	12	98.6%	0.205	12	98.3%	0.202	13
DAC ^α	1000	36.0%	0.292	11	55.0%	0.276	11	80.2%	0.278	11	94.5%	0.283	10
DAC ^α	12000	2.5%	0.937	1	2.9%	0.924	1	4.7%	0.914	1	12.3%	0.907	1
DM-Codec ^β	500	98.7%	0.295	12	104.6%	0.264	12	107.1%	0.264	12	105.8%	0.283	12
DM-Codec ^β	1000	33.9%	0.479	9	53.0%	0.447	9	77.4%	0.435	9	97.1%	0.415	9
DM-Codec ^β	4000	3.9%	0.737	5	6.4%	0.689	6	14.4%	0.647	6	38.5%	0.595	6
SpeechTokenizer ^γ	500	15.2%	0.334	9	33.9%	0.324	9	64.2%	0.301	9	91.7%	0.277	10
SpeechTokenizer ^γ	2000	7.3%	0.773	8	16.3%	0.734	8	39.4%	0.682	8	73.8%	0.600	8
SpeechTokenizer ^γ	4000	4.4%	0.864	2	8.1%	0.822	4	21.0%	0.765	4	49.2%	0.684	5
BigCodec ^δ	1040	10.1%	0.829	7	17.8%	0.785	7	33.5%	0.718	7	63.0%	0.625	6
Mimi ^ε	1000	5.1%	0.804	6	7.8%	0.772	5	14.7%	0.726	4	33.6%	0.673	4
S3 token ^ζ	600	3.9%	0.860	2	5.2%	0.841	2	8.1%	0.815	2	16.7%	0.779	3
TASTE (ours)	~150	4.8%	0.842	4	5.3%	0.830	3	6.9%	0.815	2	11.1%	0.792	1

^α Kumar et al. (2023); ^β Ahsan et al. (2025); ^γ Zhang et al. (2024); ^δ Xin et al. (2024b); ^ε Défossez et al. (2024); ^ζ Du et al. (2024a)

884 A.1.4 ROBUSTNESS ABLATION ON TASTE TOKENIZER

885 To evaluate our tokenizer robustness, we have conducted controlled noise level experiments on speech
 886 reconstruction. Specifically, we add 4 different levels of white noise to the original waveform and
 887 then evaluate the reconstruction performance. The noise levels are defined by signal-to-noise ratio
 888 (SNR) ranging from 20dB (almost clean) to 5dB (very noisy). We report two metrics: ASR-WER as
 889 an indicator of reconstruction quality, and speaker similarity (Sim.) as a measure of reconstruction
 890 similarity. For ease of comparison, we also provide the overall rank of each tokenizer considering
 891 both metrics. The results in Table 8 show that our tokenizer remains stable across different noise
 892 levels, demonstrating strong robustness. Notably, TASTE achieves the best ASR-WER under the
 893 noisiest condition. This suggests that the underlying ASR system is not a limiting factor for the
 894 general applicability of TASTE; rather, it serves as an effective and reliable source of semantic
 895 information for the reconstruction.

897 A.1.5 DETAILS ON SALMON AND STORYCLOZE

898 Our detailed results on SALMON and StoryCloze are reported in Table 9. The introductions of the
 899 two benchmarks—SALMON and StoryCloze—are described below.

900 **SALMON for Acoustic Evaluation** SALMON offers a comprehensive set of metrics designed
 901 to evaluate SLMs in multiple dimensions. In summary, each test sample consists of a *positive*
 902 sample and a *negative* sample. The *negative* sample differs from the *positive* sample by having some
 903

904 Table 9: The evaluation results on SALMON and StoryCloze of different SLMs, and BG means
 905 background. We report likelihood-based accuracy on SALMON (acoustic aspect) and StoryCloze
 906 (semantic aspect). The baseline (S3 token) is conducted by joint speech-text modeling with the S3
 907 token as speech tokenization.

METHOD	LoRA	SALMON (ACOUSTIC CONSISTENCY)					STORYCLOZE	
		Sentiment	Speaker	Gender	Room	BG (domain)	BG (rand.)	sSC / tSC
<i>Previous Work</i>								
TWIST 1.3B ((Hassid et al., 2023))	✗	61.5±3.4	69.0±3.3	69.5±3.3	59.0±3.5	55.5±3.5	60.5±3.5	52.4±0.8 / 70.6±0.7
TWIST 7B ((Hassid et al., 2023))	✗	61.5±3.4	71.0±3.2	70.0±3.2	62.0±3.4	55.5±3.5	60.5±3.5	55.3±0.8 / 74.1±0.7
Spirit LM ((Nguyen et al., 2025))	✗	54.5±3.5	69.5±3.3	67.0±3.3	54.5±3.5	53.5±3.5	55.5±3.5	61.0±0.8 / 82.9±0.6
Spirit LM Expr. ((Nguyen et al., 2025))	✗	73.5±3.1	81.0±2.8	85.0±2.5	54.5±3.5	56.0±3.5	64.0±3.4	56.9±0.8 / 75.4±0.7
<i>Ours</i>								
Baseline (S3 token)	✓	49.5±3.5	48.8±3.5	48.8±3.5	49.5±3.5	55.3±3.5	49.5±3.5	54.4±0.8 / 63.0±0.8
TASLM 1B (token)	✓	59.0±3.5	68.0±3.3	70.5±3.2	61.0±3.4	52.0±3.5	54.0±3.5	64.2±0.8 / 88.9±0.5
TASLM 1B (embedding)	✓	57.5±3.5	67.0±3.3	75.5±3.0	50.0±3.5	47.0±3.5	49.0±3.5	64.0±0.8 / 89.5±0.5

918 segments altered. These alterations include changes in speaker, gender, environment (e.g., room
919 acoustics), or sentiment in the middle of the utterance. The SLM serves as an anomaly detector that
920 aims to distinguish between the pairs of *positive* and *negative* samples. The distinction is based on
921 the likelihood score given by each SLM, which is then evaluated with the overall precision between
922 the ground truth and the prediction.

923
924 **StoryCloze for Semantic Evaluation** To evaluate the SLMs’ ability to comprehend semantic
925 coherence and logical reasoning, we employ the spoken version of StoryCloze test (sSC) and the
926 Topic StoryCloze test (tSC) assembled by Hassid et al. (2023). Assessment of narrative understanding
927 involves presenting a four-sentence story setup, followed by two possible endings. These tasks require
928 the model to select the most appropriate conclusion, thereby testing its grasp of causal and temporal
929 relationships within a narrative. Similarly to SALMON, we measure the accuracy of the distinctions
930 based on the likelihood scores.

931
932 **Discussion on SALMON and StoryCloze** On SALMON, we observe that our TASLM falls short
933 for background-related attributes (Room, Background) where the samples are added with environmental
934 sounds (echoes, instruments, background noises from FSD50K). Since TASTE tokenization
935 focuses on natural speech and has not been trained on audio with environmental sound and noise, it
936 may not be able to convey such information. However, on the speech related attributes, such as gender
937 and speaker, our TASLM performs much better and is comparable to other SLMs. On StoryCloze,
938 our TASLM successfully retains its semantic capability with effective joint modeling on TASTE,
939 leading to the best results among all pretrained SLMs.

940 A.1.6 REPORT OF STANDARD DEVIATIONS

941 We report the standard deviations of our tables in the main text to allow further investigation.

943 Table 10: Results with standard deviations of Table 1

945 Method	946 Bitrate	947 QUALITY				948 SIMILARITY		
		949 WER ↓	950 UTMOS	951 DNSMOS	952 ViSQOL	953 Drtn. Con.	954 Spkr. Sim.	955 MUSHRA
956 Ground Truth	957 256k	958 2.1%±0.07	959 4.09±0.32	960 3.84±0.26	961 -	962 -	963 -	964 76.6±15.9
965 Encodec (Défossez et al., 2023)	966 1500	967 5.1%±0.11	968 1.58±0.34	969 3.26±0.24	970 3.46±0.28	971 0.94±0.003	972 0.63±0.10	973 -
	974 3000	975 2.6%±0.08	976 2.35±0.53	977 3.48±0.25	978 3.81±0.27	979 0.96±0.002	980 0.78±0.07	981 25.6±18.6
982 SpeechTokenizer (Zhang et al., 2024)	983 500	984 5.2%±0.11	985 1.27±0.05	986 2.99±0.17	987 2.80±0.24	988 0.94±0.003	989 0.35±0.09	990 -
	991 2000	992 3.0%±0.08	993 3.56±0.43	994 3.60±0.28	995 3.65±0.22	996 0.97±0.002	997 0.80±0.06	998 53.9±22.9
	999 4000	1000 2.5%±0.08	1001 3.90±0.36	1002 3.76±0.28	1003 4.03±0.17	1004 0.98±0.002	1005 0.92±0.04	1006 -
1007 Mimi (Défossez et al., 2024)	1008 1000	1009 3.1%±0.09	1010 3.60±0.37	1011 3.60±0.30	1012 3.62±0.26	1013 0.96±0.002	1014 0.82±0.06	1015 67.6±19.8
1016 S3 token (topline) (Du et al., 2024a)	1017 600	1018 3.0%±0.09	1019 4.18±0.27	1020 3.90±0.24	1021 3.30±0.26	1022 0.96±0.002	1023 0.82±0.09	1024 70.2±17.0
1025 Text-only (baseline)	1026 ~50	1027 5.9%±0.11	1028 4.31±0.16	1029 4.11±0.22	1030 2.44±0.23	1031 0.57±0.006	1032 0.78±0.09	1033 42.6±27.1
1034 TASTE (ours)	1035 ~150	1036 4.4%±0.11	1037 4.29±0.18	1038 4.10±0.22	1039 3.05±0.26	1040 0.91±0.003	1041 0.80±0.08	1042 68.3±17.1

956 Table 11: Results with standard deviations of Table 2.

957 Method	958 Finetuned / base 959 parameters	960 CONTINUATION			961 LIKELIHOOD		
		962 GPT-4o	963 UTMOS	964 Human	965 SALMON	966 StoryCloze	967 Overall
<i>Cascade</i>							
1000 Cascade (LLaMA3.2-1B ^α)	-	1001 3.15±1.27	1002 4.25±0.22	1003 4.00±1.28	-	-	-
1004 Cascade (LLaMA2-7B ^β)	-	1005 3.43±1.27	1006 4.25±0.25	1007 3.98±1.29	-	-	-
<i>Spoken LMs</i>							
1008 TWIST 1.3B (Hassid et al., 2023)	1009 1.3B / 1.3B ^θ	1010 1.48±0.70	1011 3.25±0.48	1012 1.95±1.01	1013 62.5±1.4	1014 61.5±0.5	1015 62.0±0.7
1016 TWIST 7B (Hassid et al., 2023)	1017 7B / 7B ^θ	1018 1.44±0.70	1019 3.27±0.52	1020 2.04±0.91	1021 63.4±1.4	1022 64.7±0.5	1023 64.1±0.7
1024 Spirit LM (Nguyen et al., 2025)	1025 7B / 7B ^θ	1026 2.79±1.06	1027 3.41±0.19	1028 2.38±0.81	1029 59.1±1.4	1030 72.0±0.5	1031 65.6±0.7
1032 Spirit LM Expr. (Nguyen et al., 2025)	1033 7B / 7B ^θ	1034 1.90±1.03	1035 3.40±0.30	1036 2.41±0.96	1037 69.0±1.3	1038 66.2±0.5	1039 67.6±0.7
1040 Baseline (S3 token)	1041 45M / 1.3B ^α	1042 1.37±0.87	1043 4.04±0.27	1044 2.84±1.11	1045 50.2±1.4	1046 58.7±0.6	1047 54.5±0.8
1048 TASLM 1B (token)	1049 45M / 1.3B ^θ	1050 3.08±1.37	1051 4.07±0.28	1052 3.93±1.30	1053 60.8±1.4	1054 76.5±0.5	1055 68.7±0.7
1056 TASLM 1B (embed.)	1057 45M / 1.3B ^θ	1058 3.16±1.33	1059 4.22±0.21	1060 4.16±1.20	1061 57.7±1.4	1062 76.7±0.5	1063 67.2±0.7

1064 Base models: ^αLLaMA3.2-1B, ^βLLaMA2-7B, ^γLLaMA-7B, ^θOPT-1.3B

1065 Table 12: Results with standard deviations of Table 3.

1066 Method	1067 Mode	1068 Web Q.	1069 LLaMA-Q.
1070 Mini-Omni 0.5B(T→T)	1071 T	1072 21.3±0.9	1073 39.0±2.8
1074 Mini-Omni 0.5B (Xie & Wu, 2024a)	1075 T+A	1076 4.5±0.5	1077 11.6±1.8
1078 Helium 7B (text)	1079 T	1080 32.3±1.0	1081 75.0±2.5
1083 Moshi 7B (Défossez et al., 2024)	1084 T+A	1085 26.6±1.0	1086 62.3±2.8
1088 LLaMA3.1-8B-Instruct	1089 T	1090 60.4±1.1	1091 71.7±2.6
1094 Llama-Omni-8B (Fang et al., 2024)	1095 T+A	1096 35.5±1.1	1097 67.3±2.7
1099 LLaMA3.2-1B[†]	1100 T	1101 24.0±0.9	1102 51.0±2.9
1104 TASLM 1B (embed.)[†]	1105 T+A	1106 27.1±1.0	1107 57.6±2.9

1108 [†]We apply few-shot learning to facilitate question answering.

972 A.2 TRAINING DETAILS
973974 A.2.1 HYPERPARAMETERS AND CONFIGURATIONS
975976 We separate the training process into the two phases: *deriving TASTE tokenization and conducting*
977 *spoken language modeling with TASTE*. In the tokenization phase, only the Aggregator, Quantizer,
978 and the UnitDecoder is trainable. We use the Adam (Kingma, 2015) optimizer and the learning rate
979 is set to 0.0016. The batch size is set to 160 seconds on each of the 8 NVIDIA A6000 GPUs we used.
980 Note that in the first 2 epochs the quantization is not applied. From the beginning of the third epoch,
981 quantization is applied and the Quantizer starts to be updated. We train the TASTE tokenizer for 5
982 epochs, which takes about 2 days for learning, with the learning rate gradually decayed.
983984 As for the spoken language modeling training phase, we use the AdamW (Loshchilov & Hutter,
985 2019) optimizer, the Cosine scheduler with the learning rate set to 1e-5. We use 8 Nvidia A6000
986 GPUs for training. The total batch size summation over the GPUs is set to 768 samples with the
987 gradient accumulation steps set to 2. To reduce the memory overhead and the computational cost, we
988 employ `bfloat16` mixed precision during training. Tools such as DeepSpeed (Rasley et al., 2020)
989 and Liger Kernel (Hsu et al., 2024) are also applied to speed up the fine-tuning process of the SLM.
990991 A.3 EVALUATION DETAILS
992993 A.3.1 HUMAN EVALUATION
994995 We conduct human listening tests through Amazon Mechanical Turk. In each experiment, we
996 randomly select the same 20 samples from each method; and for each sample we collect more than
997 10 evaluation scores across different human evaluators.
998999 **MUSHRA** In Table 1, we have shown our result of the MUSRHA human listening test (Series,
1000 2014). Following Zhang et al. (2024), we conduct the evaluation with a hidden reference but without
1001 a lowerpass-filtered anchor. We instruct evaluators to rate the perceptual quality of the given samples
1002 with respect to the ground truth on a scale of 1 to 100.
10031004 **Speech Continuation MOS** In Table 2, we mention that we have conducted the human listening
1005 test to evaluate the overall performance of the speech continuations. Here, we present the instruction
1006 for human speech continuation MOS evaluation as follows:
10071008 Instruction for Human Speech Continuation MOS Evaluation
10091010 In this test, each sample will contain a short audio clip called "prompt" (3 seconds) and a longer audio
1011 clip called "prompt+continuation" (~15 seconds).
1012 You will be asked to rate the speech quality of the "prompt+continuation" audio clip, specifically focus
1013 on the "continuation" part.
1014 The rating should be based on how likely you think that the long audio is a proper continuation of the
1015 "prompt" audio.
1016 Specifically, the rating should be based on the following scale:
10171018 1: Bad - The "continuation" is not distinguishable or not natural.
1019 2: Poor - The "continuation" is 25% distinguishable.
1020 3: Fair - The "continuation" is 50% distinguishable and natural.
1021 4: Good - The "continuation" is 75% distinguishable and natural.
1022 5: Excellent - The "continuation" is distinguishable, meaningful, and natural.
10231024 **Distinguishable** means that the words in the "continuation" is distinguishable.
1025 **Natural** means that the "continuation" sounds like a real human voice and a natural continuation of the
1026 prompt without considering the content of the speech.
1027 **Meaningful** means that you can not only distinguish the words but also understand the meaning of the
1028 whole "prompt+continuation".
1029

1026 A.3.2 GPT-4O FOR MOS EVALUATION
1027
1028

1029 As introduced in Section 5.1.2, we use GPT-4o to assign MOS scores to the speech continuation
1030 results (Chiang & Lee, 2023; Lin et al., 2024). Here, we describe the detailed procedure. First,
1031 whisper-large-v3 is applied to transcribe the generated speech. Then, given the transcription,
1032 the text content from the prompt audio, and the instruction template, GPT-4o can produce a score
1033 between 1 and 5. The instruction template is provided below:

1034
1035
10361037 Instruction Prompt for GPT-4o MOS Evaluation
1038

1039 The task is evaluating the relevance and likelihood of the
1040 predicted text continuation, given the text prompt. You should
1041 also consider whether the meaning of the text continuation is
1042 making sense. The text prompt is:

1043 "`{prompt}`"
1044 , and the text continuation is :
1045 "`{content}`"

1046
1047 You must give an overall rating from 1 to 5. The rating guideline
1048 is as below:

1049 1: The text continuation is very unlikely and irrelevant to the
1050 text prompt.
1051 2: The text continuation is unlikely and marginally relevant to
1052 the text prompt.
1053 3: The text continuation is moderately likely and relevant to the
1054 text prompt.
1055 4: The text continuation is likely and relevant to the text
1056 prompt.
1057 5: The text continuation is very likely and highly relevant.

1058 You should take the following steps to provide the score:
1059 First: briefly analyze the sample with the above definition.
1060 Second: MUST follow the output format as: I would rate the score
1061 as _

1062
1063
10641065
1066 A.4 TACKLING THE VOCABULARY MISMATCH
1067

1068

1069 The vocabulary mismatch problem lies in the fact that the vocabulary sets are different between the
1070 ASR and the LLM, and TASTE is aligned with the text transcription tokens from ASR. Consider
1071 that given a text transcription v and the vocabulary sets of ASR and LLM denoted as \mathbb{V}^{asr} and \mathbb{V}^{llm} ,
1072 the ASR tokenized sequence $v^{\text{asr}} = [v_1^{\text{asr}}, v_2^{\text{asr}}, \dots, v_N^{\text{asr}}]$, $v_i^{\text{asr}} \in \mathbb{V}^{\text{asr}}$ and the LLM tokenized sequence
1073 $v^{\text{llm}} = [v_1^{\text{llm}}, v_2^{\text{llm}}, \dots, v_M^{\text{llm}}]$, $v_i^{\text{llm}} \in \mathbb{V}^{\text{llm}}$ can be different in terms of token ids and sequence lengths.
1074 Since the TASTE token and embedding are aligned with v^{asr} , we need to derive a method to align
1075 them with v^{llm} for text-aligned speech-text modeling. Notice that v^{asr} and v^{llm} both represent v ,
1076 we propose to mitigate the issue through word-level *grouping*, *averaging*, and *aligning*, detailed
1077 in Algorithm 1. By crafting TASTE speech tokenization into the word level, we are able to align
1078 it with the text tokens of the LLM, denoted as \tilde{q}, \tilde{z} . In practice, we also adopt the word-level
1079 averaging technique during the TASTE tokenization training phase, ensuring that the word-level
TASTE tokenization facilitates high-quality reconstruction.

1080 **Algorithm 1** Aligning TASTE with LLM Tokenization via Word-Level Techniques

1081 1: **Initialization:**

1082 Text transcription $v = [\text{word}_1, \text{word}_2, \dots, \text{word}_W]$

1083 ASR tokens of the transcription $v^{\text{asr}} = [v_1^{\text{asr}}, v_2^{\text{asr}}, \dots, v_N^{\text{asr}}]$

1084 TASTE embedding $\hat{z} = [\hat{z}_1, \hat{z}_2, \dots, \hat{z}_N]$

1085 LLM tokens of the transcription $v^{\text{llm}} = [v_1^{\text{llm}}, v_2^{\text{llm}}, \dots, v_M^{\text{llm}}]$

1086 2: **procedure** WORDLEVELGROUPING($v, v^{\text{asr}}, \hat{z}, v^{\text{llm}}$)

1087 3: Since v^{asr} is a token sequence represents v , we can easily group it by words:

1088 4: $v^{\text{asr}}_{\text{grouped}} \leftarrow [(\underbrace{v_1^{\text{asr}}, v_2^{\text{asr}}, v_3^{\text{asr}}}_1, \underbrace{v_4^{\text{asr}}}_2, \dots, \underbrace{v_{N-1}^{\text{asr}}, v_N^{\text{asr}}}_W)]$ \triangleright Group v^{asr} by the words of v

1089 5: With the word-level grouping from $v^{\text{asr}}_{\text{grouped}}$, we can group TASTE embedding \hat{z} as well:

1090 6: $\hat{z}_{\text{grouped}} \leftarrow [(\hat{z}_1, \hat{z}_2, \hat{z}_3)_1, (\hat{z}_4)_2, \dots, (\hat{z}_{N-1}, \hat{z}_N)_W]$

1091 7: Finally, we can group v^{llm} following the similar procedure of grouping v^{asr} :

1092 8: $v^{\text{llm}}_{\text{grouped}} \leftarrow [(\underbrace{v_1^{\text{llm}}, v_2^{\text{llm}}}_1, \underbrace{v_3^{\text{llm}}, v_4^{\text{llm}}}_2, \dots, \underbrace{v_{M-2}^{\text{llm}}, v_{M-1}^{\text{llm}}, v_M^{\text{llm}}}_W)]$

1093 9: Due to the *vocabulary mismatch*, the grouping of $v^{\text{llm}}_{\text{grouped}}$ is different from $v^{\text{asr}}_{\text{grouped}}, \hat{z}_{\text{grouped}}$.

1094 10: **end procedure**

1095 11: **procedure** WORDLEVELAVERAGING(\hat{z}_{grouped})

1096 12: $\bar{z} \leftarrow []$ \triangleright Initialize a new sequence

1097 13: **for** word group index $i \leftarrow 1$ to W **do**

1098 14: word group $(\hat{z}_j, \dots, \hat{z}_k) \leftarrow \hat{z}_{\text{grouped}}[i]$

1099 15: $\bar{z}_{[j:k]} \leftarrow \text{Average}((\hat{z}_j, \dots, \hat{z}_k))$ \triangleright Average the word group

1100 16: **append** $\bar{z}_{[j:k]}$ **to** \bar{z}

1101 17: **end for**

1102 18: Resulting in word-level TASTE embedding $\bar{z} \in \mathbb{R}^{W \times d_z}$, where W is the word length of v .

1103 19: **end procedure**

1104 20: **procedure** ALIGNWORDLEVELEMBEDDINGWITHLLM($\bar{z}, v^{\text{llm}}_{\text{grouped}}$)

1105 21: $\tilde{z} \leftarrow []$ \triangleright Initialize a new sequence

1106 22: **for** word group index $i \leftarrow 1$ to W **do**

1107 23: word group $(v_j^{\text{llm}}, \dots, v_k^{\text{llm}}) \leftarrow v^{\text{llm}}_{\text{grouped}}[i]$

1108 24: $M \leftarrow \text{Length}((v_j^{\text{llm}}, \dots, v_k^{\text{llm}}))$ \triangleright Get the length of the word group.

1109 25: **for** $m \leftarrow 1$ to M **do** \triangleright add $M \times \bar{z}[i]$ into the aligned sequence \tilde{z}

1110 26: **append** $\bar{z}[i]$ **to** \tilde{z}

1111 27: **end for**

1112 28: **end for**

1113 29: **end procedure**

1114 30: **return** The LLM-aligned word-level TASTE embedding \tilde{z} and its codes form \tilde{q}

1117

1118 **A.5 THE WEIGHTED SUM MECHANISM FOR MODALITY FUSION**

1119

1120 The speech decoder takes the text-aligned speech embedding \hat{z} and the text embedding v as input

1121 conditions. As depicted in Figure 2, in practice we perform a *weighted sum* mechanism to obtain the

1122 final fused embedding z_{joint} . The weights to fuse the two modalities are represented by two learnable

1123 parameters, denoted as w_{sp} and w_{txt} . The whole process of modality fusion can be denoted as follows:

1124 $\hat{z}', v' = \text{normalize}(\hat{z}), \text{normalize}(v), [p_{\text{sp}}, p_{\text{txt}}] = \text{softmax}([w_{\text{sp}}, w_{\text{txt}}]), z_{\text{joint}} = p_{\text{sp}} \cdot \hat{z}' + p_{\text{txt}} \cdot v'$.

1125

1126 **A.6 DISCUSSION ON THE USAGE OF LLM**

1127

1128 We discuss our usage of LLM following the conference’s policy. We use an AI assistant (ChatGPT

1129 specifically) to polish English prose, including grammar correction, wording refinements, consistent

1130 terminology and hyphenation, and minor restructuring for clarity and flow. The assistant suggests

1131 alternative phrasings, section bridges, and standard disclosure/impact wording based on author-

1132 provided content. It does not generate novel ideas, claims, analyses, figures, code, or results, and it

1133 does not access proprietary data. All technical content and conclusions are our own, and we review

and edit all AI-assisted text and take full responsibility for the final manuscript.